DOI: 10.1002/chem.200902817

A Rigid Dinuclear Ruthenium(II) Complex as an Efficient Photoactive Agent for Bridging Two Guanine Bases of a Duplex or Quadruplex Oligonucleotide

Stéphane Rickling,[a] Liana Ghisdavu,[a] Frédéric Pierard,[a] Pascal Gerbaux,[b] Mathieu Surin,[c] Pierre Murat,[d] Eric Defrancq,[d] Cécile Moucheron,[a] and Andrée Kirsch-De Mesmaeker*[a]

Abstract: The rigid dinuclear $[(tap)_2Ru(tpac)Ru(tap)_2]^{4+}$ complex (**1**) (TAP = 1,4,5,8-tetraazaphenanthrene, TPAC = tetrapyridoacridine) is shown to be much more efficient than the mononuclear bis-TAP complexes at photodamaging oligodeoxyribonucleotides (ODNs) containing guanine (G). This is particularly striking with the G-rich telomeric sequence $d(T_2AG_3)_4$. Complex **1**, which interacts strongly with the ODNs as determined by surface plasmon resonance (SPR) and emission anisotropy experiments, gives rise under illumination to the formation of covalent adducts with the G units of the ODNs. The yield of photocrosslinking of the two strands of duplexes by **1** is the highest when the G bases of each strand are separated by three to four base pairs. This corresponds with each $Ru(tap)_2$ moiety of complex **1** forming an adduct with the G base. This separation distance of the G units of a duplex could be determined thanks to the rigidity of complex **1**. On the basis of results of gel electrophoresis, mass spectrometry, and molecular modelling, it is suggested that such photocrosslinking can also occur intramolecularly in the human telomeric quadruplex $d(T_2AG_3)_4$.

Keywords: DNA · N ligands · oligonucleotides · photochemistry · ruthenium

Introduction

Mononuclear Ru^{II} complexes containing at least two 1,4,5,8-tetraazaphenanthrene (TAP) or 1,4,5,8,9,12-hexaazatriphenylene (HAT) ligands are known to give rise to a photo-induced electron transfer in the presence of an electron donor such as a guanine (G) base.[1,2] Moreover, these Ru compounds are capable of crosslinking covalently two complementary oligodeoxyribonucleotide (ODN) strands, provided that each strand contains at least one G base, separated from each other by no or one base pair. However, the yield of this photoreaction is rather low because the crosslinking requires two successive absorptions of a photon by the same Ru species. Thus, an adduct of the Ru complex on a G base of one strand is produced by a first photon absorption and afterwards the same Ru compound forms a covalent bond with a G unit of the complementary strand by a second photon absorption. These two steps give rise to the bridging of the two ODN strands.[3]

With the aim of exploring novel targets for these photocrosslinkings and also improving these photoinduced double anchoring processes, we studied an a priori more appropriate Ru complex, namely the dinuclear $[(tap)_2Ru(tpac)Ru(tap)_2]^{4+}$ complex (**1**, TPAC = tetrapyridoacridine). The photophysical and electrochemical properties of this compound suggest that it should act as an efficient photocrosslinking agent for the following reasons.[4] Firstly, the photophysical properties of **1** are almost the same as those of mononuclear

[a] Dr. S. Rickling, Dr. L. Ghisdavu, Dr. F. Pierard, Prof. C. Moucheron, Prof. A. Kirsch-De Mesmaeker
Organic Chemistry and Photochemistry, Université libre de Bruxelles
50 avenue F.D. Roosevelt, 1050 Bruxelles (Belgium)
Fax: (+32) 2-650-3018
E-mail: akirsch@ulb.ac.be

[b] Dr. P. Gerbaux
Laboratoire de Chimie Organique
Centre de Spectrométrie de Masse, Université de Mons
20 Place du Parc, 7000 Mons (Belgium)

[c] Dr. M. Surin
Laboratory for Chemistry of Novel Materials, Université de Mons
20 Place du Parc, 7000 Mons (Belgium)

[d] P. Murat, Prof. E. Defrancq
Département de Chimie Moléculaire
UMR CNRS 5250 Université Joseph Fourier BP 53
38041 Grenoble cedex 9 (France)

Supporting information for this article is available on the WWW under http://dx.doi.org/10.1002/chem.200902817.

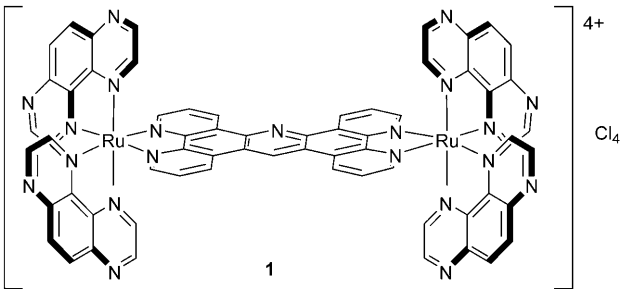

1

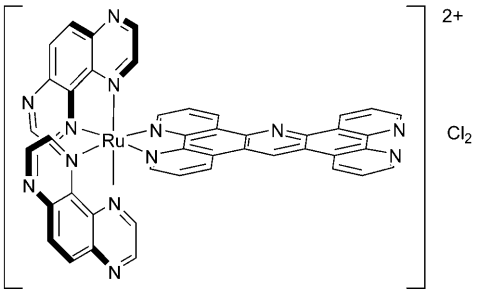

2

$[Ru(tap)_2(tpac)]^{2+}$ complex (**2**),[4] and the first electrochemical oxidation of **1** appears at the same potential as that of **2**, corresponding to a two-electron process involving the two Ru centres. This suggests that the two metallic centres behave independently in spite of the conjugated TPAC bridging ligand. Secondly, complex **1** has an oxidizing power in its ^{3}MLCT (metal-to-ligand charge transfer) excited state[4] similar to that of the mononuclear bis-TAP complexes mentioned above. Under illumination, **1** should thus also be able to extract one electron from a guanine base and give rise to an adduct of the metallic species to the G moiety as observed, for example, with $[Ru(tap)_2(phen)]^{2+}$ (Figure 1).[3,5] Moreover, due to the presence of the two Ru metallic centres and the four TAP ligands in **1**, the probability of obtaining more than one photoadduct on the same complex **1** should increase and improve the photocrosslinking.

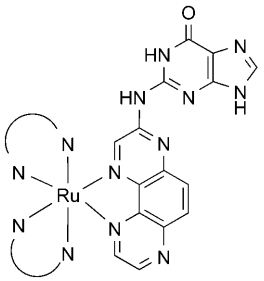

Figure 1. Structure of the photoadduct of a Ru complex containing at least two TAP ligands with a guanine base.

On the other hand, the photocrosslinking processes would be of great interest in case of guanine-rich DNA sequences. Such sequences are known to form highly ordered structures called G-quadruplexes, because of the association of planar G quartets of four guanine residues held together by eight Hoogsteen-type hydrogen bonds.[6] These structures have been found to play an important role in many relevant biological processes such as telomere stabilisation, oncogene activation and regulation of the immunoglobulin switch region.[7] The design of small molecules that can bind and stabilise the folded G-quadruplex conformation has received much attention, because these nucleic acid motifs represent valuable pharmaceutical targets.[8] Thus it would be particularly interesting to damage these sequences by intramolecular photobridging of two or more G bases by using the metallic species **1**. Indeed, this photoinduced bridging process would "freeze" the folded G-quadruplex conformation.

In this work we use **1** as a photocrosslinking agent with ODN duplexes, and we compare its behaviour with the properties of mononuclear bis-TAP and bis-HAT Ru complexes. We report on the interaction and photoreaction of complex **1** with the human telomeric sequence $d(T_2AG_3)_4$, which is known to form G-quadruplex structures.[6,9]

Results and Discussion

Emission of complex 1: As a first step, we examined the quenching of the emission of **1** by calf thymus DNA (CT-DNA) and the human telomeric sequence $d(T_2AG_3)_4$. Emission anisotropy was also measured to assess the mobility of complex **1** in its excited state, in interaction with CT-DNA and the $d(T_2AG_3)_4$ sequence.

Luminescence quenching of ***1***: The ratios I/I_0 (I = the emission intensity for different P/Ru ratios [equivalents of phosphate]/[complex **1**] and I_0 = the emission intensity in the absence of polynucleotide) were plotted as a function of increasing ODN concentration for a constant concentration of **1** (Figure 2). The I/I_0 values do not depend on the time passed in the dark before each emission measurement, showing that the interaction equilibrium between complex **1**

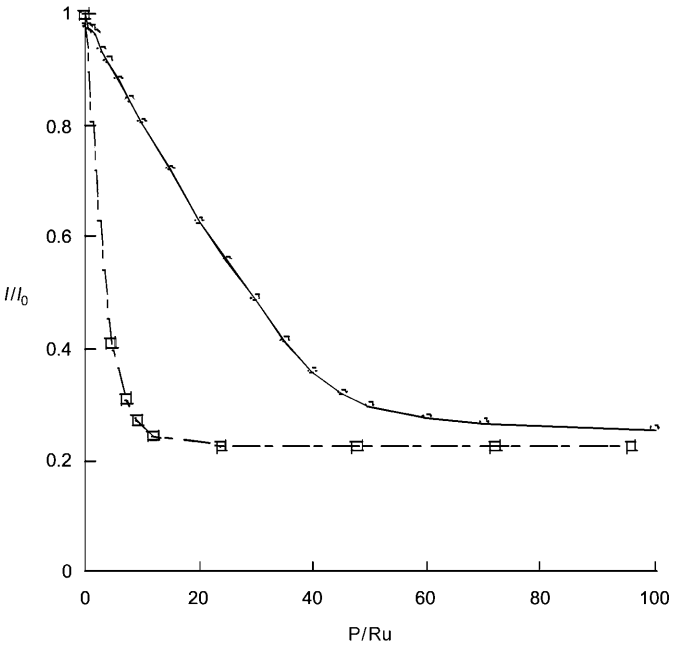

Figure 2. Ratios I/I_0 for a constant concentration of **1** (5 μM) plotted as a function of the ratio P/Ru = [phosphate]/[**1**], with 10 mM cacodylate buffer, 80 mM NaCl, pH 7.0; circles: titration with CT-DNA; squares: titration with the human telomeric sequence $d(T_2AG_3)_4$.

and the two types of DNA is reached within a minute. Data revealed important luminescence quenching by the polynucleotides. The values I/I_0 at the plateau correspond to the situation in which the total amount of **1** interacts with the polynucleotide. They reflect the content in G bases, thus in emission quenchers. As expected, the emission of **1** is more efficiently quenched by the telomeric $d(T_2AG_3)_4$ sequence than by CT-DNA. Taking into account the value of the reduction potential of **1**,[4] its luminescence can indeed be efficiently quenched by electron transfer from the G bases.

*Emission anisotropy of complex **1** in the presence of polynucleotides*: By measuring the emission anisotropy under polarised light, we can investigate the mobility/immobility of complex **1** during its excited state lifetime while interacting with DNA. The anisotropy (r) of the ^{3}MLCT emission of complex **1**, as defined in the experimental section, was measured in the absence and in the presence of CT-DNA or the telomeric sequence $d(T_2AG_3)_4$ in a buffer/glycerol mixture (50:50) at +12 °C. The values of r are collected in Table 1, together with those of $[Ru(tap)_2(phen)]^{2+}$ (phen = 1,10-phenanthroline) as well as with values reported in the literature for other Ru^{II} complexes interacting with DNA.

Table 1. Anisotropy (r) data in the absence and presence of CT-DNA or $d(T_2AG_3)_4$.[a]

Complex	r (without CT-DNA)	r (with CT-DNA)	r (with $d(T_2AG_3)_4$)
$[Ru(bpy)_2(dppz)]^{2+}$ [b]	–	0.048	
$[Ru(bpy)_3]^{2+}$ [b]	0.0007	0.004	
$[Ru(tap)_2(phen)]^{2+}$ [c]	0.002	0.020	
$[(tap)_2Ru(tpac)Ru(tap)_2]^{4+}$ (**1**)	0.001	0.049	0.012

[a] The measurements were performed under the following conditions, unless it is specified otherwise: The concentration of the complexes was 2.5 μM in a water/glycerol mixture (50:50) containing 10 mM cacodylate buffer (pH 7.0) and 80 mM NaCl at +12 °C. When present, the CT-DNA and $d(T_2AG_3)_4$ concentration was 187.5 μM in phosphate equivalents. The samples were excited at 450 nm and the emission was measured between 500 and 800 nm. Abbreviations: phen = 1,10-phenanthroline, bpy = 2,2′-bipyridine, dppz = dipyrido[3,2-*a*:2′,3′-*c*]phenazine. [b] The anisotropy (r) values calculated from the polarisation (P) values reported in the literature {[Ru] = 10 μM, [DNA] = 1 mM, 20 mM sodium phosphate buffer (pH 7.85), 10 mM NaCl/glycerol (40:60)}. [c] Measurements of samples in a water/glycerol mixture (50:50) containing 10 mM cacodylate buffer (pH 7.0), but no NaCl was added; this was to favour the binding of this complex, which has a much lower affinity for DNA than **1**.

While the emission of **1** is almost completely depolarised in buffer solution containing 50 % glycerol, an increase of emission anisotropy is observed in the presence of CT-DNA. The r value of **1** is comparable to that reported for the thoroughly studied metallo-intercalator $[Ru(bpy)_2(dppz)]^{2+}$ (bpy = 2,2′-bipyridine; dppz = dipyrido[3,2-*a*:2′,3′-*c*]phenazine).[10] In contrast, the retention of anisotropy with $[Ru(tap)_2(phen)]^{2+}$, the luminescence of which is also quenched by electron transfer and has luminescence lifetimes similar to those of **1** in the presence of DNA,[11] is significantly lower than that observed for **1**. This indicates that the high anisotropy value of **1** in the presence of CT-DNA reflects a high degree of immobilisation of **1**. This would be consistent with the intercalation of this dinuclear complex. However, dinuclear complexes connected through their intercalating dppz moieties through a flexible,[12] a semi-rigid[13] or a rigid linker[14] have all been shown to intercalate through an extremely slow threading mechanism requiring large conformational changes of DNA. The absence of kinetic processes before reaching the equilibrium interaction (see above) indicates that **1** does not thread one of its bulky $Ru(tap)_2$ moieties through the base pairs stack of DNA to intercalate its planar bridging TPAC ligand. The significant retention of emission anisotropy of **1** upon DNA binding is therefore proposed to result from a groove binding of this large dinuclear complex (see also discussion of molecular modelling below).

In the presence of the telomeric sequence $d(T_2AG_3)_4$, the anisotropy values of **1** are lower than those measured with CT-DNA. A faster rotational diffusion of the quadruplex $d(T_2AG_3)_4$ when compared to CT-DNA, due to its much smaller size and different shape, most probably accounts for this decrease of anisotropy. The emission retains, however, significant polarisation in the presence of the telomeric sequence, and this indicates that **1** is held in a relatively rigid environment when bound to the G quartet.

Interaction of 1 with oligonucleotides: The affinity constants of **1** for the duplex and quadruplex forms were measured by surface plasmon resonance (SPR) analyses. Moreover, molecular modelling was performed to examine the possible binding geometries.

For the SPR experiments, we used the telomeric sequence $d(T_2AG_3)_4$ and a GC-rich duplex. These two sequences were anchored on streptavidin-coated surfaces through a biotinylated cyclodecapeptide (see Experimental Section).[15] From these SPR data (see Supporting Information) we found that **1** exhibits a good affinity for both systems. The affinity constants were, indeed, estimated to be $7.6\times10^6\,M^{-1}$ for the telomeric sequence $d(T_2AG_3)_4$ and $2.9\times10^6\,M^{-1}$ for the GC-rich duplex.

Earlier molecular modelling and experimental studies of the DNA-binding geometry of structurally related dinuclear complexes showed that the bridging ligand tpphz (tetrapyridophenazine), which has the same dimension as TPAC, is not long enough to allow the corresponding dinuclear complex to span the base pairs stack of DNA.[16] Instead, this complex was proposed to bind to DNA through adsorption in the major groove,[16] a binding mode also proposed for a large dinuclear ruthenium(II) triple-stranded helicate.[17] The molecular modelling for **1** suggests that its intercalation through the DNA grooves is also very unlikely, because the distance between the hydrogen atoms of the two TAP ligands on the same Ru^{II} centre is 10.6 Å, that is, around three times the distance between adjacent π-stacking base pairs in DNA. Moreover, intercalation by threading does not accord with the binding equilibrium being reached within the minute (vide supra). Complex **1** can accommodate the pocket formed by the major groove (process often

referred to as "adsorption") with almost no change in the B-helix DNA structure (Figure 3A).[18] Quadruplex structures, such as human telomere $d(T_2AG_3)_4$, offer a broad range of interaction geometries: in addition to groove binding and core intercalation, other interaction modes, such as end pasting and loop interaction, have also been reported.[19] If we consider an end-pasting mode (i.e., docking of the complex on top of a G quartet),[20,21] from our simulations we observe that the size and shape of **1** would accommodate the size of a quartet, but the loops (the DNA backbone surrounding the quartet sheets) leave no sufficient space to adsorb, neither on the top, nor at the bottom of the three sheets of G4. Instead, **1** can interact in the grooves formed by neighbouring loops at the four sides of the telomeric sequence perpendicularly to the plane of the G4 sheets (Figure 3B). In the telomeric sequence, there are two small grooves, one middle-size groove and one wide groove. The width of the small groove is too small for **1** to interact with the guanine residues. The other two grooves are large enough to accommodate **1** with the TPAC plane perpendicular to the guanine sheets (Figure 3B shows a plausible interaction along the wide groove). This makes possible hydrogen-bond formation between the nonchelated nitrogen atoms of the TAP and the amino hydrogen of the guanine pointing outwards at the periphery of the telomeric sequence.

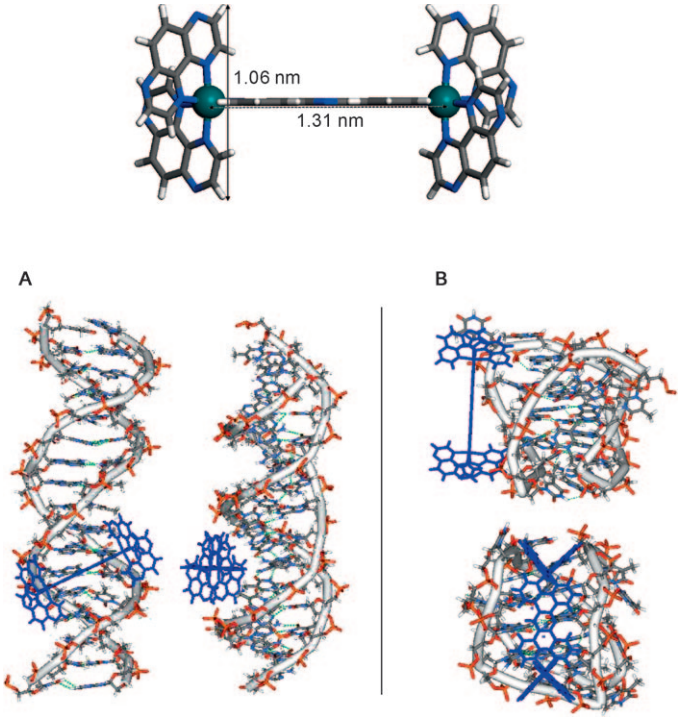

Figure 3. "Stick" molecular models shown from different view axes of the interaction of **1** (in dark blue): A) along the major groove of a duplex DNA and B) between the intramolecular grooves of the "143D" telomere quadruplex structure. The backbones are shown as grey tubes. Distances for complex **1** are also indicated.

Photoreaction of 1 with G-containing ODNs: The emission quenching of **1** by CT-DNA and the telomeric sequence is accompanied by the formation of photoproduct(s), as evidenced by changes of the absorption spectrum after illumination (see Supporting Information). Moreover, after dialysis of the illuminated solution in the presence of CT-DNA or the telomeric sequence, the MLCT absorption band in the visible region is still present with a λ_{max} shifted into the blue direction when compared to that of the starting complex (see Supporting Information). This indicates that the photoproduct(s) corresponds to covalent adducts on these sequences.[22]

With G-containing duplexes: The photoreaction of **1** was first examined in the presence of different ODN duplexes containing one guanine (G) base on each strand. Therefore, a series of 17-mer ODN duplexes **ds0–ds6** were prepared. They differ by the number of base pairs between the G's on each strand, going from zero to six base pairs (Table 2). Table 2 also gives the distances between the amino groups of the two G's for each duplex, as calculated by molecular modelling.

As the photoproducts correspond to adducts of complex **1** on the G bases of the oligonucleotides, gel electrophoresis

Table 2. The different ODN duplexes studied in the presence of 80 mM NaCl after 15 min illumination.

	Sequence	Distance[a] [Å]	ODN [%] Starting material	Photo-adduct	Photocross-linking[b]
ds0	5′TTT.TC**G**.TTT.TAA.ATT.TA3′ 3′AAA.AG**C**.AAA.ATT.TAA.AT5′	3.9	26	68	6
ds1	5′TTT.TTT.TCT.**G**AA.ATT.TA3′ 3′AAA.AAA.AG**A**.CTT.TAA.AT5′	7.6	32	56	12
ds2	5′TTT.TTT.TCT.AG**A**.ATT.TA3′ 3′AAA.AAA.AG**A**.TCT.TAA.AT5′	11.3	42	47	11
ds3	5′TTT.TTT.CTT.AG**A**.ATT.TA3′ 3′AAA.AAA.**G**AA.TCT.TAA.AT5′	14.8	33	42	25
ds4	5′TTT.TTC.TTT.AG**A**.ATT.TA3′ 3′AAA.AA**G**.AAA.TCT.TAA.AT5′	18.1	30	43	27
ds5	5′TTT.TCT.TTT.AG**A**.ATT.TA3′ 3′AAA.AG**A**.AAA.TCT.TAA.AT5′	21.3	36	47	17
ds6	5′TTT.TCT.TTT.AA**G**.ATT.TA3′ 3′AAA.AG**A**.AAA.TTC.TAA.AT5′	24.4	40	43	17

[a] Distance [Å] between the amino groups of the two G's for each duplex, as calculated from molecular modelling. [b] For the determination of the percentages, we did not take into account the intensity of the spots that migrate a little less than the photoadduct (very weak intensity). Moreover, the percentages represent averaged values for 3–4 experiments after 15 min illumination (see also Supporting Information, Figure S4).

experiments were performed to detect these adducts as a function of the illumination time of **1** in the presence of each duplex. These polyacrylamide gel electrophoresis (PAGE) experiments were performed under denaturing conditions. The bands should thus correspond to single strands, and those migrating less rapidly than the starting material could be attributed to adducts of **1** on the single-strand ODN (photoadducts) or to photocrosslinking. In addition, to determine the distance of migration corresponding to a duplex, that is, two strands migrating together under denaturing conditions and corresponding to a photocrosslinking by complex **1**, we deposited on the gel a 17-mer duplex ODN with a chemically attached photoreactive Ru complex, before and after illumination (Figure 4, lanes 15 and 16). We

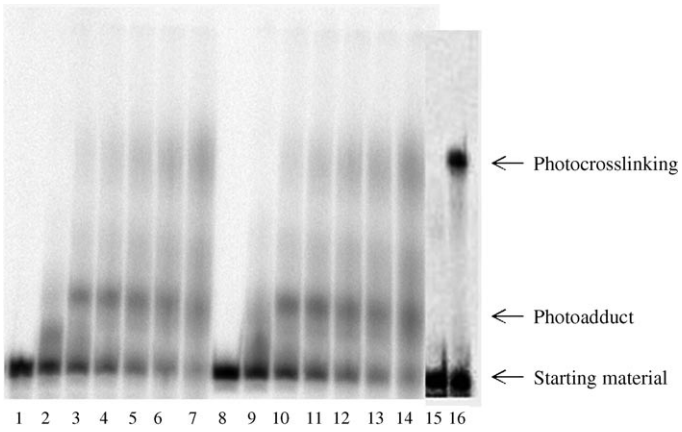

Figure 4. Gel electrophoresis analysis (20% denaturing polyacrylamide gel) of **ds3** and **ds4** (55 μM) and complex **1** (15 μM) in 10 mM sodium cacodylate buffer, 80 mM NaCl, at pH 7, and with illumination with the He/Cd laser at 442 nm. Lane 1: non-illuminated **ds3**; Lane 2: non-illuminated **ds3** with **1**; Lane 3: **ds3** with **1** after 4 min illumination; Lane 4: **ds3** with **1** after 8 min illumination; Lane 5: **ds3** with **1** after 12 min illumination; Lane 6: **ds3** with **1** after 16 min illumination; Lane 7: **ds3** with **1** after 30 min illumination; Lane 8: non-illuminated **ds4**; Lane 9: non-illuminated **ds4** with **1**; Lane 10: **ds4** with **1** after 4 min illumination; Lane 11: **ds4** with **1** after 8 min illumination; Lane 12: **ds4** with **1** after 12 min illumination; Lane 13: **ds4** with **1** after 16 min illumination; Lane 14: **ds4** with **1** after 30 min illumination. Lane 15: non-illuminated Ru-derivatised duplex; Lane 16: Ru-derivatised duplex after 30 min illumination.

showed in the past that after illumination of this duplex chemically derivatised by $[Ru(tap)_2(dip)]^{2+}$ (DIP = 4,7-diphenylphenanthroline), the two strands become irreversibly photocrosslinked.[23] Consequently, the spot in Figure 4, lane 16 constitutes a reference for the photocrosslinking process between two 17-mer ODNs. If complex **1** is able to photocrosslink the different duplexes, a spot with the same electrophoretic mobility as that of the Ru-derivatised duplex in lane 16 is thus expected.

A representative result of a gel electrophoresis analysis is shown in Figure 4. The smears accompanying the spots are due to adsorption of **1** on single strands (or double strands).[24] This adsorption seems to cause a splitting in two of the migrating ODN bands (Figure 4, lanes 2 and 9; see also Supporting Information, Figure S4, lanes 10, 14 and 18 before illumination) and makes attribution of the spots more difficult. However it is clear (see also Supporting Information, Figures S4 and S5) that new spots have appeared with illumination. The spots designated "photoadduct" are attributed to the covalent adducts of complex **1** on the ODN. This attribution is made by comparison with the known behaviour of the other photoreactive bis-TAP complexes studied up to now in the presence of G-containing ODN.[1,2] The spots that migrate as in lane 16 (Figure 4; see also Supporting Information, Figure S4, lane 22), that is, as the two 17-mer ODNs covalently linked by a mononuclear complex, are attributed to the photoproducts resulting from the photocrosslinking of the two ODNs through complex **1**. The percentages of the bands for the starting ODN, photoadduct and photocrosslinking collected in Table 2 represent the average of the values determined from three to four experiments. As shown in Table 2 for the illumination of 15 minutes, the maximum of photocrosslinked strands is obtained for **ds3** and **ds4** (25% and 27%, respectively), in which the inter-guanine distances are 14.8 and 18.1 Å, respectively (i.e., 3 and 4 base pairs).

For **ds3** and **ds4**, the evolution of the intensity of the spots has also been measured as a function of the illumination time (Figure 4); the corresponding percentages are collected in Table 3. After a short period of illumination (4 min), the

Table 3. Percentages of photoadduct formation for complex **1** with **ds3** and **ds4** in the presence of 80 mM NaCl as a function of the illumination time with the He/Cd laser at 442 nm.

Duplex	*t* [min]	Unreacted [%]	Photoadduct [%]	Photocrosslinking [%]
ds3	0	100	0	0
ds3	4	64	30	6
ds3	8	53	36	11
ds3	12	45	38	17
ds3	16	38	38	24
ds3	30	28	35	37
ds4	0	100	0	0
ds4	4	65	30	5
ds4	8	52	36	12
ds4	12	43	38	19
ds4	16	37	38	25
ds4	30	25	38	37

adduct of **1** on one strand represents already 30% and the photocrosslinking accounts only for 6% of the total radioactivity. With increasing illumination time, the photoadduct first increases and afterwards remains more or less constant, whereas the photocrosslinking increases steadily. This behaviour suggests that the photoadduct is first produced and the absorption of light by this compound leads to the crosslinking process of the two strands.

According to the structure of the photoadduct determined previously with the bis-TAP complexes (Figure 1), the photoreactive positions generating the adduct on the TAP ligand are in the α-positions of the nonchelating nitrogen atoms. From the molecular modelling of **1**, there are eight possibilities for the distances between the carbon atoms in

the α-positions of the nitrogen atoms of the different TAP units belonging to the opposite metal centres (the two α-carbon atoms on one TAP of the first metal centre with the four α-carbon atoms of two TAPs of the second metal centre): 12.6, 15.5, 17.0 (3 times), 17.2, 19.9, and 20.5 Å. Therefore, there are five chances out of eight to have photoreactions at two TAP reactive sites separated by distances of 15.5–17.2 Å. These distances correspond to those separating the amino nitrogen atoms of the two G's of **ds3** and **ds4** (14.8 and 18.1 Å respectively, Table 2) that lead to the highest percentage of photocrosslinking. This result also affords strong support to a binding mode by adsorption in the duplex grooves (see Figure 4A). The photocrosslinking observed with zero or one base pair between the two G's probably corresponds to a photocrosslinking by two TAP ligands belonging to the same Ru ion of **1**.

With the telomeric sequence: Taking into account the high photoreactivity of **1** towards the G-containing ODNs, we tested the photoreactions with the telomeric sequence $d(T_2AG_3)_4$. For this purpose, gel electrophoresis experiments were carried out under denaturing conditions after illumination of **1** in the presence of the $d(T_2AG_3)_4$ quadruplex form (see Experimental Section). Figure 5 shows the gel electrophoresis analysis for complex **1** illuminated as a function of time in the presence of the telomeric sequence $(T_2AG_3)_4$, when a [telomere phosphate]/[**1**] ratio of 3.66 is used. It is very interesting that after only 3 minutes (lane 3), 75–80% of the starting sequence (>90% after 6 min and 9 min) has already disappeared. This is extremely rapid compared to the photoreaction on ODNs achieved in the past under similar conditions with mononuclear bis-TAP complexes,[23] and currently with the $[Ru(tap)_2(tpac)]^{2+}$ complex (**2**). In this last case, under the same conditions, only 18% of the starting telomeric sequence was photodamaged after illumination for 3 minutes (see Supporting Information, Figure S5). This shows that dinuclear complex **1** is much more efficient, and consequently that the high percentage of photodamage is not caused solely by the telomeric sequence being rich in G units. Moreover, as shown in Figure 5, complex **1** in contrast to complex **2** (Supporting Information, Figure S5) gives rise to the appearance of five to six new spots, the sixth spot being visible in the starting well. The different photoproducts **a**–**f** detected with **1** could be attributed to the irreversible addition of one to six complexes **1** on the oligonucleotide sequence. Because complex **1** has a 4+ charge, the 24 negative charges of the 24-mer single-strand telomeric sequence should be neutralised after the addition of six complexes, which could explain the presence of a nonmigrating spot remaining in the starting well.

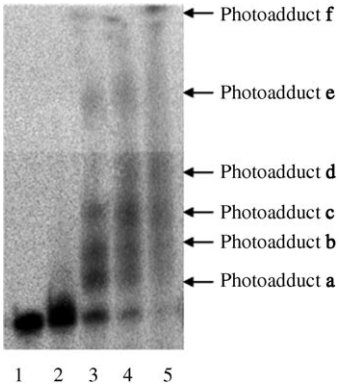

Figure 5. Gel electrophoresis analysis of the reaction mixture of the telomeric sequence $(T_2AG_3)_4$ (55 μM) and **1** (15 μM) in 10 mM cacodylate buffer, 80 mM NaCl, at pH 7, and with illumination with the He/Cd laser at 442 nm. Lane 1: non-illuminated sequence; Lane 2: non-illuminated sequence in the presence of **1**; Lanes 3–5: crude reaction mixture of telomeric sequence and **1**, after 3, 6, and 9 min of illumination, respectively. For lane 3, the approximate percentages of each photoadduct are: 28 (**a**), 26 (**b**), 16 (**c**), and 13% (**e**); photoadducts **d** and **f** are not measured.

During the first minutes of illumination (Figure 5, lane 3) the different photoadducts already appear and, as a function of the illumination, the faster migrating adducts decrease in favour of the nonmigrating band (photoadduct **f**). Although it is clear that several photoadducts are formed, these results do not indicate whether complex **1** bridges two guanine bases of the sequence. To check this possibility and prove the existence of covalent adducts, we analysed a solution of **1**, illuminated with the telomeric sequence, by nano-electrospray mass spectrometry. For these experiments, other illumination conditions were used (see experimental section) and the resulting solutions were dialysed and analysed by gels. They indicated mainly the presence of photoproducts **a**–**c**, without **d**–**f**.

The recorded mass spectrum of this dialysed solution, presented in Figure 6, reveals the presence of different cationic species that can be readily identified on the basis of the measured mass-to-charge ratios, provided the charge state of each detected ion is first identified. This was achieved by

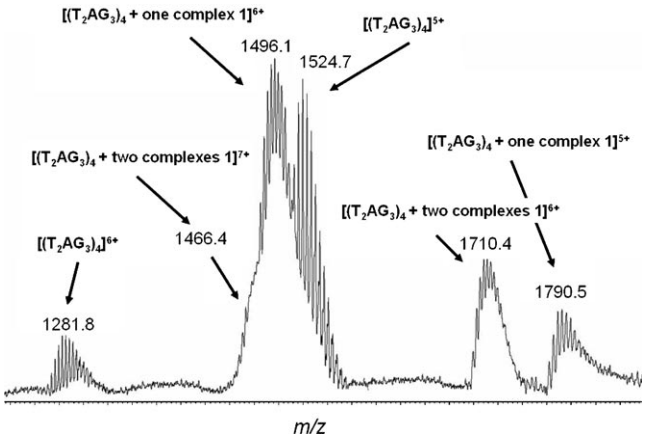

Figure 6. Mass spectrometric analysis of the "telomere/complex **1**" solution after irradiation: nano-ESI mass spectrum (positive ion mode) of the crude reaction mixture after dialysis, evaporation, and dissolution in aqueous ammonium acetate (50 mM). Values correspond to the most abundant species inside each distribution.

measuring the *m/z* difference between two adjacent signals inside each distribution. It is worth remembering that each distribution in the spectrum arises from progressive replacements of one proton by one sodium ion ($\Delta MW = 22$ u.)

As expected, signals corresponding to the starting telomeric sequence $d(T_2AG_3)_4$ are observed at *m/z* 1281.8 and 1524.7 and are readily attributed to sixfold- and fivefold-charged cations, $[(T_2AG_3)_4+1H^++5Na^+]^{6+}$ and $[(T_2AG_3)_4+3H^++2Na^+]^{5+}$, respectively, for the most abundant species inside each distribution. More interestingly, the mass spectrum also reveals the existence of covalent adducts of **1** on the telomeric sequence after illumination. We clearly identify ions arising from the covalent addition of one and two complexes on the oligonucleotide sequence. The corresponding ions are detected at *m/z* 1496.1 (6+) and 1790.5 (5+), for [$(T_2AG_3)_4$+one complex **1**], and at *m/z* 1466.4 (7+) and 1710.4 (6+), for [$(T_2AG_3)_4$+two complexes **1**] (see below for the adjustment of the resulting charge with Na^+ and/or H^+ cations).

Upon irradiation, the telomeric sequence gains thus one and two complexes **1** and, according to the structure of the adduct of one TAP complex on a G base (Figure 1), this addition process should be accompanied by the loss of one molecule of hydrogen per one covalent bond formation. Consequently, in the case of the addition of one complex **1** to the sequence, [$(T_2AG_3)_4$+one complex **1**], a confirmation by mass spectrometry of the number of covalent bond(s) inside this adduct (one or two) relies on the determination of a 2 u or 4 u difference when compared to the noncovalent interaction of $d(T_2AG_3)_4$ with one complex **1** (thus not photochemically attached).[25] The results are still more complicated if two complexes of **1** would form covalent adducts on the telomeric sequence (each adduct with one or two covalent bonds formed). In such a case, there can be differences of 4, 6, or 8 u compared to noncovalent interactions between $d(T_2AG_3)_4$ and two complexes of **1**. Whether there are covalent bonds between complex **1** and $d(T_2AG_3)_4$ or not is thus confirmed by only minute differences or equalities between the experimental and calculated *m/z* values for different possibilities of covalent adducts. The calculated *m/z* values for noncovalent interactions and covalent adducts with an increasing number of covalent bonds are presented in Table 4; the formula correspond to the species obtained by (noncovalent and covalent) interaction between one complex **1** or two complexes of **1** and the telomeric sequence. They do not include the required adjustment of the mass and charge by the required number of proton or sodium atoms. Thus, the initial charge of the species, if the counteranions are not considered, is evidently defined by the number of Ru cations in the formula. Consequently, from an eight-charged species (addition of two complexes **1**), for example, the corresponding six-charged cations detected upon ESIMS analysis are obtained by the removal of two protons. Those protons are likely to originate from the phosphodiester groups constituting the skeleton of the ODN sequence. In the same way, the replacement of hydrogen atoms by sodium atoms can be realised without modification of the charge of the detected ions, but, of course, with modification of the mass due to the sodium atoms.

Table 4. Different bindings (noncovalent and covalent) between complex **1** and the telomeric sequence for the addition of one or two complexes **1** to the $(T_2AG_3)_4$ telomere with the predicted mass-to-charge ratios.

$(T_2AG_3)_4$ + one complex **1**		
Type of interaction	Formula[a]	Calcd *m/z*[b]
noncovalent	$C_{305}H_{334}N_{117}O_{146}P_{23}Ru_2$	(6+) 1496.565
1 covalent bond	$C_{305}H_{332}N_{117}O_{146}P_{23}Ru_2$	(6+) 1496.213
2 covalent bonds	$C_{305}H_{330}N_{117}O_{146}P_{23}Ru_2$	(6+) 1495.877
$(T_2AG_3)_4$ + two complexes **1**		
Type of interaction	Formula[a]	Calcd *m/z*[c]
noncovalent	$C_{370}H_{371}N_{138}O_{146}P_{23}Ru_4$	(6+) 1711.255
1 covalent bond	$C_{370}H_{369}N_{138}O_{146}P_{23}Ru_4$	(6+) 1710.919
2 covalent bonds	$C_{370}H_{367}N_{138}O_{146}P_{23}Ru_4$	(6+) 1710.583
3 covalent bonds	$C_{370}H_{365}N_{138}O_{146}P_{23}Ru_4$	(6+) 1710.247
4 covalent bonds	$C_{370}H_{363}N_{138}O_{146}P_{23}Ru_4$	(6+) 1709.911

[a] Formula corresponding to the telomere plus one or two complexes **1** (thus, charges 4+ or 8+) without covalent and with covalent bond formation and without explicit addition or elimination of H^+ or Na^+ for the charge adjustment (see text). [b] Calculated *m/z* ratio for a sixfold-charged cation containing four sodium cations. [c] Calculated *m/z* ratio for a sixfold-charged cation containing three sodium cations.

In the case of the [$(T_2AG_3)_4$+one complex **1**] species, as depicted in Figure 6, the more intense peak distribution observed corresponds to the sixfold charged ions, with *m/z* 1496.088 (1496.1) as the base peak. As potential formula for these corresponding 6+ ions, we can consider three different possibilities, which are presented in Table 4. This comparison (experimental versus calculated data) definitely rules out the occurrence of a noncovalent interaction, because the corresponding *m/z* ratio would be much larger than the experimental value. This shows also that the dialysis treatment is efficient, and unambiguously confirms the covalent nature of the binding between complex **1** and the telomeric sequence. We can thus confirm that at least one covalent bond is formed between both partners. Unfortunately, this does not allow us to conclude that an intramolecular photocrosslinking has formed. Nevertheless, given that the measured *m/z* ratio is intermediate between the calculated *m/z* values for both covalent species (that with one covalent bond and that with two covalent bonds), it is reasonable to propose that a mixture of both covalent species was generated.

As far as the [$(T_2AG_3)_4$+two complexes **1**] species is concerned (thus with an initial charge of 8+), the most abundant ion observed in the mass spectrum of Figure 6 is detected at *m/z* 1710.365 (1710.4), and is identified as a sixfold-charged cation containing three sodium ions (thus $-5H^+$ and $+3Na^+$). Several possibilities have to be considered to account for the experimental *m/z* ratio. In the present case, not less than five possibilities were calculated, and the theoretical values are listed in Table 4. Again, the measured *m/z* ratio that amounts to 1710.365 confirms the covalent nature of the interaction, because the corresponding *m/z* ratio of the noncovalent adduct (1711.255) is much larger than the experimental value. Moreover, the measured data

of *m/z* 1710.365 lies between *m/z* 1710.247 and *m/z* 1710.583. This indicates 1) the occurrence of at least one covalent bond per complex (a total of two covalent bonds for the species) and 2) most probably the appearance of three covalent bonds in the species containing the telomeric sequence with two complexes. Thus, at least one of the covalently bound complexes would have photobridged two G's of the sequence. The presence of a mixture of different covalent species (two covalent and three covalent bonds) can explain the mass spectrometry data.

On the basis of these results, we performed molecular modelling of the intramolecular photocrosslinking of the telomeric sequence by **1**. We considered that covalent bonds occur between the carbon α to the nonchelating nitrogen of one TAP and the nitrogen of the guanine amino group. Such modelling is made easier thanks to the rigidity of the TPAC ligand and the resulting complex **1**. Thus, starting from the configuration shown in Figure 3B, in which **1** accommodates the wide groove of the telomeric sequence, we covalently linked **1** to the telomere and carried out molecular dynamics (MD) simulation. At 298 K on the 2 ns timescale, we observed that **1** has no tendency to intercalate through the G quartet, and remains on the periphery, outside the loop as shown in Figure 7, corresponding to the last

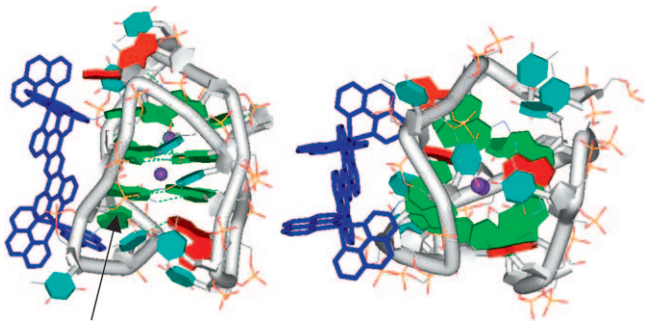

Figure 7. Structure of the last snapshot of the 2 ns MD run of **1** covalently linked to the 143D telomere $d(T_2AG_3)_4$ (structure based on data in reference [9a]). Complex **1** is shown in dark blue, the sugar phosphate skeleton as a gray tube, Na^+ in purple, G in green, A in red, T in pale blue, and the hydrogen bonds as dashed green lines. The models are shown with the quartet sheets almost perpendicular (left) and parallel (right) to the view (hydrogen atoms are omitted for the sake of clarity).

snapshot of the MD (see Supporting Information, Figure S6). The telomeric structure in the three sheets of G4 is globally maintained, although from time to time in the MD one G is no longer hydrogen bonded to the other G of one quartet (see, e.g., one G shown by the black arrow in Figure 7, see also Supporting Information, Figure S7). The DNA backbone loops are slightly different from the initial structure, but globally the anti-parallel shape of the loops is maintained and the Na^+ ions remain in between these sheets, centred in the square formed by each G quartet.

Conclusion

Our results demonstrate clearly that compound **1** may be considered as the most efficient photoreactive bis-TAP Ru complex, forming covalent adducts with the G bases of ODNs in duplexes or quadruplex forms. A combination of favourable factors explains this photoreactivity. A strong interaction of **1** with the ODNs as concluded from the SPR and retention of anisotropy data constitute a prerequisite for this photoreactivity. Moreover, the bridging ligand TPAC, in spite of its planar and conjugated character, does not behave as a good coupling agent of the electronic properties of the two metal centres, so that each Ru centre keeps its own excited state properties, that is, the capability of electron extraction from G bases, which induces the formation of covalent bonds and adducts. After a first photon absorption and an adduct formation, this new species is able in its turn to produce a second adduct with another G base after a second photon absorption, and induces in this way a photocrosslinking between two base units.

Concerning the experiments performed with the ODN duplexes, the higher yield of photocrosslinking when the two G bases are separated by three to four base pairs is in agreement with the above conclusion, according to which each $Ru(tap)_2$ centre of complex **1** plays an independent role. As the TPAC ligand is quite rigid, as is the resulting complex **1**, the calculation of the distances between the two Ru reactive moieties can be estimated and compared to the distances separating the two photocrosslinked G's in the duplex. This calculation agrees perfectly with the experimental results concerning the photocrosslinking. These interesting results with the duplexes also stress the advantages of using complex **1** as a rigid molecular ladder for measuring the best distance between 2 G units to reach the highest efficiency of photocrosslinking by **1**.

The photodamaging effect of complex **1** is particularly impressive towards the quadruplex $d(T_2AG_3)_4$. As explained above, this is most probably due to reabsorption of photons by a same dinuclear species. Actually, complex **1** should be able to photocrosslink several G bases of a same telomeric sequence. As already discussed, this is difficult to demonstrate. However, we have several arguments in favour of this hypothesis. If we take into account that the MS data unambiguously indicate that more than one complex **1** is covalently bound to one telomeric sequence, this means that the local concentration of photoadducts on the ODN is high, which favours absorption of light by these species and thus favours the photocrosslinking. The detailed analysis of the MS results indicates the existence of such processes. In addition, the photocrosslinkings of the ODN strands in duplexes by **1** also support this hypothesis, and the molecular modelling simulations of the "quadruplex complex **1**" species without and with covalent bond formations are also compatible with our conclusions. Such intramolecular photocrosslinkings could block the activity of the telomerase because the telomere's unfolding would no longer be possible, which could lead to interesting biomedical applications.

Experimental Section

Materials and products: $[Ru(tap)_2(tpac)]Cl_2$ (**2**) and dinuclear $[(tap)_2Ru(tpac)Ru(tap)_2]Cl_4$ (**1**) complexes were synthesised according to procedures previously described.[4] The 17-mer ODNs were prepared by automated DNA synthesis on an ABI 3400 DNA synthesiser (Applied Biosystem) by use of standard β-cyanoethylphosphoramidite chemistry on a 1 μmol scale. For the Ru-labelled ODN used as reference (see below), the $[Ru(tap)_2(dip)]^{2+}$ complex (DIP = 4,7-diphenylphenanthroline derivatised by a linker) was attached to the 5′-end of ODN according to procedures previously described.[23] The ODNs were purified by PAGE, by using *tris*-borate/ethylenediaminetetraacetic acid (TBE) buffer and urea (7 M). The double stranded ODNs were prepared by heating the radioactively labelled strands with their complementary strands to 90 °C for 5 min, and then allowing them to return at room temperature overnight.

The human telomeric sequence $d(T_2AG_3)_4$ was purchased from Eurogentec (Liège, Belgium). The sequence was dissolved in buffered aqueous solutions containing Na^+ ions, heated to 95 °C for 10 min, and left overnight at room temperature before use. Denaturing curves for the sequence $d(T_2AG_3)_4$ ($c = 6$ μM) were determined in 10 mM sodium cacodylate and 80 mM NaCl at pH 7.0, from two temperature cycles going from 80 °C to 10 °C and vice versa (see Supporting Information). The melting temperature corresponded to 47 °C and was increased by 2 °C in the presence of 1.5 μM of complex **1** (see Supporting Information). The T4 polynucleotide kinase was purchased from Pharmacia Biotech and the [γ-^{32}P]ATP from Amersham. Urea was purchased from Bio-Rad, acrylamide from Acros, 1 M tris(hydroxymethyl)aminomethane hydrochloride (Tris-HCl), pH 7.0, boric acid, adenosine 5′-phosphosulfate sodium salt (APS), *N,N,N′,N′*-tetramethylethylenediamine (TEMED), and ethylenediaminetetraacetic acid (EDTA) from Sigma. Glycerol (99.5+ % spectrophotometric grade) used for the anisotropy experiments was purchased from Janssen Chimica (Belgium).

5′-End-labelling reactions: The human telomeric sequence $d(T_2AG_3)_4$ and the 17-mer ODNs were 5′-end-labelled by using T4 polynucleotide kinase and [γ-^{32}P] ATP at 37 °C for 30 min. Electrophoresis Blue (10 μL) was added to 5 μM aqueous solutions of the double-stranded ODN (or telomeric sequence) prior to deposition on the gel. The photoreaction products were separated by migration on a 20% denaturing (7 M urea) polyacrylamide gel (acrylamide/bisacrylamide = 19:1) by using TBE buffer (90 mM tris-borate, 2 mM EDTA, pH 8.0). In the case of the duplex containing the attached $[Ru(tap)_2(dip)]^{2+}$ complex, the non-Ru-labelled strand of the duplex was ^{32}P-labelled at the 5′ extremity.

Photoreactions: The changes of absorption due to the photoreactions were followed as a function of the illumination time of the Ru complexes (with a He/Cd laser, 30 mW, Melles Griot, excitation wavelength = 442 nm) in the presence of different ODNs at room temperature. Typically, a 10 μL solution containing the Ru complex (15 μM) and ODN (single strand or duplex) or human telomeric sequence $d(T_2AG_3)_4$ (55 μM in base-equivalents) with 10 mM sodium cacodylate and 80 mM NaCl buffer at pH 7.0, was illuminated. For the MS analyses, the photoreactions were carried out by irradiating a 300 μL sample containing complex **1** (45 μM) and human telomeric sequence $d(T_2AG_3)_4$ (165 μM) with 10 mM sodium cacodylate and 80 mM NaCl buffer at pH 7.0. Under these conditions, an illumination time of 15 min was chosen, so that the faster-migrating spots (i.e., photoadducts **a**, **b**, and **c** in Figure 5, see above) could be easily detected by gel electrophoresis analysis. After dialysis, evaporation, and dissolution in aqueous ammonium acetate, the thus obtained solution was immediately subjected to the nano-ESI analysis.

Instrumentation: The absorption spectra were recorded on a Perkin–Elmer Lambda 40 UV/Vis spectrophotometer. The emission spectra were obtained on a Shimadzu RF-5001PC spectrofluorimeter equipped with a Hamamatsu R928 red-sensitive photomultiplier tube for detection and a 250-W Xe lamp as excitation source. The electrophoresis gels were exposed to a Phosphor Imager screen overnight at −80 °C. The gels were visualised by a Phosphor Imager Storm 860 instrument (Amersham Pharmacia Biotech).

Mass spectrometry: The illuminated samples of complex **1** with sequence $d(T_2AG_3)_4$ were dialysed three times consecutively during 1 h against a 2 M NH_4Cl solution, then three times consecutively during 1 h against deionised water. The cellulose dialysis membrane with a cut-off of 6.6–8 KD was purchased from Bioblock. Water was evaporated by using a speed vacuum and the residue was dissolved in a 50 mM ammonium acetate solution (pH 6.9) to achieve an approximate 50 μM oligonucleotide concentration. The solution was immediately subjected to the MS analysis. MS measurements were performed on a Waters QToF2 apparatus equipped with an orthogonal nano electrospray ionisation (nano-ESI) source (Z-spray) operating in positive ion mode. Sample solutions were directly injected into the ESI source from Proxeon NanoES capillaries. Typical ESI conditions consisted of the following: capillary voltage 1.0 kV, cone voltage 100 V, extractor voltage 5 V, source temperature 80 °C, and desolvation temperature 120 °C. Dry nitrogen was used as the ESI gas. The quadrupole was set to pass ions from 100 to 3000 Th and the ions were transmitted into the pusher region of the time-of-flight analyser for mass analysis with 1 s integration time. Data were acquired in continuum mode until acceptable average data were obtained.

Emission anisotropy: Emission anisotropy data were obtained by the L-format method by using an Edinburgh Instruments FS-900CDT steady-state spectrophotometer (Edinburgh Instruments, UK) equipped with a 450 W xenon lamp as excitation source and a Peltier-cooled Hamamatsu R955 red-sensitive photomultiplier for detection. All the measurements were temperature controlled with a thermostated circulating bath.

The samples were excited at 450 nm and the emission was collected between 500 and 800 nm (with a Coherent-Ealing 495 nm cut-off filter) with a constant band width of 10.4 nm. Glan Thompson (calcite) polarisers were used for both the excitation and emission light, and the anisotropy (r) of the emitted light was calculated by using Equation (1)[26]

$$r = \frac{I_{VV} - I_{VH(c)}}{I_{VV} + 2I_{VH(c)}} \quad (1)$$

in which I_{IJ} are the intensities integrated over the frequencies of the luminescence spectra recorded with different polarisations, the first subscript describing the excitation polariser position (vertical (V) or horizontal (H)) and the second the emission polariser position. $I_{VH(c)}$ is the integration of the corresponding emission spectrum corrected for the different sensitivities of the detection system for vertically and horizontally polarised light as shown in Equation (2):

$$I_{VH(c)} = I_{VH}\frac{I_{HV}}{I_{HH}} \quad (2)$$

The samples consisted of 2.5 μM ruthenium complex in a water/glycerol mixture (50:50) containing 10 mM cacodylate buffer (pH 7.0) and 80 mM NaCl. When present, the CT-DNA as well as the $d(T_2AG_3)_4$ sequences were used at a concentration of 187.5 μM phosphate equivalents (phosphate/complex = 75) to ensure complete displacement of the binding equilibrium towards the bound species. The circular dichroism (CD) spectrum of CT-DNA in the mixture of buffered aqueous solution/glycerol (50:50) was recorded, and showed the typical CD signature of B-form DNA (a positive band centred at 275 nm, a negative band at 240 nm, and the intersection with the abscissa axis at 259 nm).[27] The CD spectrum of $d(T_2AG_3)_4$ recorded under the same conditions contained positive peaks at 245 and 295 nm and a negative band at 265 nm, in agreement with the single strand ODN folding into an antiparallel G-quartet structure.[28] These CD measurements confirm that the secondary structures of both CT-DNA and $d(T_2AG_3)_4$ are retained in the solvent mixture used for anisotropy measurements.

SPR measurements with ODNs and complex 1: The SPR measurements were performed on a BIAcore T100 instrument (BIAcore AB, Sweden) operated with BIAcore T100 Software 1.1. The experiments were carried out at 25 °C, and by using a working buffer (W.B.) consisting of an aqueous solution of 10 mM HEPES, pH 7.4, 100 mM NaCl, 100 mM KCl, and 3 mM EDTA with 0.05% (v/v) surfactant P_{20}. The different oligonucleotides were immobilised on a Streptavidin-coated surface (SA sensor chip,

BIAcore AB). The quadruplex ODN consisted of $d(T_2AG_3)_4$ and the duplex ODN was composed of an oligonucleotide forming a hairpin structure d(5'GCGCGCGCTTTTGCGCGCGC3'). These oligonucleotides were anchored through their 3′-extremities on a peptidic scaffold possessing a biotin residue for immobilisation on the Streptavidin surface.[15] After conditioning of the surface with a 1 min injection of a 0.2 M NaOH/5 M NaCl solution, the ODNs were injected at 2 $\mu L\,min^{-1}$ until a final response of 437 RU (response units) and 445 RU was obtained for quadruplex and duplex ODNs, respectively. Binding experiments were conducted at 30 $\mu L\,min^{-1}$ by injection of **1** dissolved in the W.B. at concentrations from 50 to 500 nM (injection time 120 s, dissociation time 500 s). Regeneration of the surface was achieved by two successive injections (120 s, 30 $\mu L\,min^{-1}$) of 10 mM glycine·HCl (pH 2.0). A nonmodified channel (i.e., a channel in which the peptidic scaffold without attached ODNs was anchored via the biotin residue) was used as reference. Curves obtained on the reference surface were subtracted from the curves recorded during the recognition process, allowing elimination of refractive index changes (due to buffer effects) and corrections of the nonspecific interactions of **1** with the Steptavidine surface (which are not negligible at high concentrations). A heterogeneous model was used to fit the experimental curves, to evaluate the affinity of **1** for the quadruplex and duplex ODNs. Equilibrium association constants for **1** were also obtained by fitting the steady-state response versus the concentration of **1** according to the Langmuir model (see Supporting Information for SPR sensorgrams and fitting using the Langmuir model).

Molecular mechanics and molecular dynamics: The structure of the dinuclear complex was obtained by DFT with B3LYP/6-31G (LANL2DZ for Ru) and constraints were imposed to maintain this geometry for subsequent MM/MD simulations. The partial charges were recalculated with the Qeq method after +2.0 charges were imposed on each Ru atom.[29] The structure of the sequence $d(T_2AG_3)_4$ is based on that described by Wang and Patel,[9a] consisting of a folded single-stranded DNA 22-mer with the sequence $d[AG_3(T_2AG_3)_3]$. The crystal structure, extracted from the RCSB Protein Data Bank (ID: 143D), corresponds to a tetraplex structure of three sheets of G quartets (G4, Figure 3B). Two thymines were added to the sequence to provide the $d(T_2AG_3)_4$ sequence, and two Na^+ ions were placed between two G4 sheets, at the centre of the square formed by the guanine bases. All the calculations were carried out by using the Discovery Studio package from Accelrys. For the duplex ODNs, the charges were assigned by the residue template, and the CHARMm force field was used (v22, modified in 2006) as it accurately describes nucleotides with small organic molecules, and has atom parameters for Ru atoms.[30] The water solvent was implicitly taken into account by the use of the generalised Born model with a simple smoothing function.[31] Several geometries and distances between complexes and DNA were tested (docking approach), and we followed the evolution of the total energy as a function of the distance.[32] Geometry optimisation was carried out by using the adopted basis Newton–Raphson algorithm with an RMS distance criterion of 10^{-2} kcal mol^{-1} Å. Molecular dynamics (MD) simulations were performed in the canonical ensemble (*N*,*V*,*T*) with a time step of 1 fs. After equilibration, MD was performed at 298 K over 2 ns, with a temperature coupling decay time of 5.0.

Acknowledgements

The authors thank the Belgian Federal Science Policy (programme IAP, P6/27) and the FRFC-FNRS (Belgian National Science Foundation) for financial support. They thank COST for supporting the collaboration between the Belgian (ULB) and French teams. They are grateful to the Nanobio program for the facilities of the Synthesis and Surface Characterisation platforms. M.S. and P.G. are Research Associates at the FNRS. P.G. is grateful to the "Fonds pour la Recherche Scientifique" (FRS-FNRS) for financial support in the acquisition of the Waters Qtof2 mass spectrometer.

[1] a) B. Elias, A. Kirsch-De Mesmaeker, *Coord. Chem. Rev.* **2006**, *250*, 1627–1641; b) C. Moucheron, *New J. Chem.* **2009**, *33*, 235–245.
[2] L. Herman, S. Ghosh, E. Defrancq, A. Kirsch-De Mesmaeker, *J. Phys. Org. Chem.* **2008**, *21*, 670–681, and references therein.
[3] L. Ghizdavu, F. Pierard, S. Rickling, S. Aury, M. Surin, D. Beljonne, R. Lazzaroni, P. Murat, E. Defrancq, C. Moucheron, A. Kirsch-De Mesmaeker, *Inorg. Chem.* **2009**, *48*, 10988–10994.
[4] B. Elias, L. Herman, C. Moucheron, A. Kirsch-De Mesmaeker, *Inorg. Chem.* **2007**, *46*, 4979–4988.
[5] A. Kirsch-De Mesmaeker, J. P. Lecomte, J. M. Kelly, *Top. Curr. Chem.* **1996**, *177*, 25–76.
[6] For general reviews on quadruplexes, see: a) J. T. Davis, *Angew. Chem.* **2004**, *116*, 684–716; *Angew. Chem. Int. Ed.* **2004**, *43*, 668–698; b) S. Neidle, S. Balasubramanian in *Quadruplex Nucleic Acids*, RSC, Cambridge, **2006**.
[7] a) A. J. Zaug, E. R. Podell, T. R. Cech, *Proc. Natl. Acad. Sci. USA* **2005**, *102*, 10864–10869; b) M. Bejugam, S. Sewitz, P. S. Shirude, R. Rodriguez, R. Shahid, S. Balasubramanian, *J. Am. Chem. Soc.* **2007**, *129*, 12926–12927; c) M. L. Duquette, P. Pham, M. F. Goodman, N. Maizels, *Oncogene* **2005**, *24*, 5791–5798.
[8] For recent reviews, see: a) A. De Cian, L. Lacroix, C. Douarre, N. Temime-Smaali, C. Trentesaux, J.-F. Riou, J.-L. Mergny, *Biochimie* **2008**, *90*, 131–155; b) D. Monchaud, M.-P. Teulade-Fichou, *Org. Biomol. Chem.* **2008**, *6*, 627–636; c) M. Franceschin, *Eur. J. Org. Chem.* **2009**, 2225–2238; d) A. Arola, R. Vilar, *Top. Med. Chem.* **2008**, *8*, 1405–1415.
[9] a) Y. Wang, D. J. Patel, *Structure* **1993**, *1*, 263–282; b) G. N. Parkinson, M. P. Lee, S. Neidle, *Nature* **2002**, *417*, 876–880.
[10] S. Delaney, M. Pascaly, P. K. Bhattacharya, K. Han, J. K. Barton, *Inorg. Chem.* **2002**, *41*, 1966–1974.
[11] A. Del Guerzo, A. Kirsch-De Mesmaeker, *Inorg. Chem.* **2002**, *41*, 938–945.
[12] B. Önfelt, P. Lincoln, B. Nordén, *J. Am. Chem. Soc.* **2001**, *123*, 3630–3637.
[13] L. Wilhelmsson, E. Esbjörner, F. Westerlund, B. Nordén, P. Lincoln, *J. Phys. Chem. B* **2003**, *107*, 1178–1179.
[14] F. Westerlund, M. Eng, M. Winters, P. Lincoln, *J. Phys. Chem. B* **2007**, *111*, 310–317.
[15] P. Murat, D. Cressend, N. Spinelli, A. Van der Heyden, P. Labbé, P. Dumy, E. Defrancq, *ChemBioChem* **2008**, *9*, 2588–2591.
[16] a) R. C. Holmberg, H. H. Thorp, *Anal. Chem.* **2003**, *75*, 1851–1860; b) D. A. Lutterman, A. Chouai, Y. Liu, Y. Sun, C. D. Stewart, K. R. Dunbar, C. Turro, *J. Am. Chem. Soc.* **2008**, *130*, 1163–1170.
[17] a) G. Pascu, A. Hotze, C. Sanchez-Cano, B. Kariuki, M. Hannon, *Angew. Chem.* **2007**, *119*, 4452–4456; *Angew. Chem. Int. Ed.* **2007**, *46*, 4374–4378, and references therein.
[18] Note that other stable geometries of interactions along the major groove are possible.
[19] a) V. Gabelica, E. S. Baker, M.-P. Teulade-Fichou, E. De Pauw, M. T. Bowers, *J. Am. Chem. Soc.* **2007**, *129*, 895–904; b) I. Ouarliac-Garnier, M.-A. Elizondo-Riojas, S. Redon, N. P. Farell, S. Bombard, *Biochemistry* **2005**, *44*, 10620–10634.
[20] I. Haq, J. Trent, B. Chowdhry, T. Jenkins, *J. Am. Chem. Soc.* **1999**, *121*, 1768–1779.
[21] J. E. Reed, A. A. Arnal, S. Neidle, R. Vilar, *J. Am. Chem. Soc.* **2006**, *128*, 5992–5993.
[22] As mentioned in the Supporting Information, drastic conditions of dialysis with 1 M NaCl are needed to desorb noncovalently bound complex **1** from the polynucleotide. After illumination, in these conditions of dialysis, **1** remains in the dialysis bag.
[23] a) O. Lentzen, J.-F. Constant, E. Defrancq, M. Prévost, S. Schumm, C. Moucheron, P. Dumy, A. Kirsch-De Mesmaeker, *ChemBioChem* **2003**, *4*, 195–202; b) S. Deroo, S. Le Gac, S. Ghosh, M. Villien, P. Gerbaux, E. Defrancq, C. Moucheron, P. Dumy, A. Kirsch - De Mesmaeker, *Eur. J. Inorg. Chem.* **2009**, 524–532.
[24] When we tested another TPAC dinuclear complex in which the TAP ligands are replaced by phenanthroline (phen) ligands, that is, with $[(phen)_2Ru(tpac)Ru(phen)_2]Cl_4$, which is not photoreactive at all to-

wards ODNs, smears accompanying the starting ODN were also observed. They cannot be avoided.
[25] Note that after the dialysis treatment (see Supporting Information), free complex **1**, thus non-photochemically attached to the ODN, should not remain in the dialysis bag.
[26] J. R. Lakowicz, *Principles of Fluorescence Spectroscopy*, 2nd ed., Kluwer Academic/Plenum, New York, **1999**.
[27] A. Rodger, B. Nordén, *Circular Dichroism and Linear Dichroism*, Oxford University Press, Oxford, **1997**.
[28] H.-Q. Yu, D. Miyoshi, N. Sugimoto, *J. Am. Chem. Soc.* **2006**, *128*, 15461–15468.
[29] A. K. Rappé, W. A. Goddard III, *J. Phys. Chem.* **1991**, *95*, 3358–3363.
[30] F. A. Momany, R. Rone, *J. Comput. Chem.* **1992**, *13*, 888–900.
[31] a) W. Im, M. S. Lee, C. L. Brooks III, *J. Comput. Chem.* **2003**, *24*, 1691–1702; b) W. Im, M. Feig, C. L. Brooks III, *Biophys. J.* **2003**, *85*, 2900–2918.
[32] D. Han, H. Wang, N. Ren, *THEOCHEM* **2004**, *711*, 185–192.

Received: October 13, 2009
Published online: February 19, 2010

